Inorg. Chem. **2002**, *41*, 4727−4731

Kinetics and Mechanism of Oxygen Atom Abstraction from a Dioxo-Rhenium(VII) Complex

JaNeille Dixon and James H. Espenson*

Department of Chemistry, Iowa State University of Science and Technology, Ames, Iowa 50011

Received November 26, 2001

The kinetics of reaction between triarylphosphanes and two newly prepared dioxorhenium(VII) compounds has been evaluated. The compounds are $MeRe^{VII}(O)_2$("O,S") in which "O,S" represents an alkoxo, thiolato chelating ligand. With $MeReO_3$, ligands derived from 1-mercaptoethanol and 1-mercapto-2-propanol form $MeRe(O)_2$(met), **2**, and $MeRe(O)_2$(m2p), **3**. These compounds persist in chloroform solution for several hours at room temperature and for 2–3 weeks at –22 °C, particularly when water is carefully excluded. They were obtained as red oils with clean ^{1}H NMR spectra, but attempts to obtain pure, crystalline products were not successful because one decomposition pathway shows a kinetic order >1. The fastest reaction occurs between P(*p*-$MeOC_6H_4)_3$ and **2**; k_{298} = 215(7) L mol^{-1} s^{-1} in chloroform at 25(1) °C. The other rate constants follow a Hammett correlation against 3σ, with ρ = –0.69(7). This study relates to oxygen atom transfer reactions catalyzed by MeReO(mtp)PPh_3, **1**, in which $MeRe(O)_2$(mtp), **4**, is a postulated intermediate that does not build up to a measurable concentration during the catalytic cycle. Compound **2** does not react with MeSTol, but MeS(O)Tol was formed when *tert*-butyl hydroperoxide was added. This suggests that equilibrium lies to the left in this reaction, **2** + MeSTol + L = MeReO(met)L + MeS(O)Tol, and is drawn to the right by a reaction between MeReO(met)L and the hydroperoxide. Triphenyl arsane does not react with **2**, but thermodynamic versus kinetic barriers were not resolved.

Introduction

The structural formulas of selected high-valent oxorhenium compounds **1**−**6** are given in Chart 1.[1−8] Compound **1** catalyzes oxygen atom transfer between two closed-shell molecules, as in YO + X → Y + XO. In that sense, the rhenium complexes can be discussed together with enzymes and enzyme mimics for biological oxygen atom transfer containing Mo[9−17] or W.[18−21] One example of a reaction catalyzed by **1** is that between pyridine *N*-oxide and triphenylphosphane.[7,22] The sequence of reactions in eqs 1−2 describes the chemistry.

$$MeRe^{V}O(mtp)L \xrightarrow[-L]{YO} MeRe^{V}O(mtp)(OY) \rightarrow MeRe^{VII}(O)_2(mtp)\ (\mathbf{4}) + Y \quad (1)$$

$$MeRe^{VII}(O)_2(mtp) \underset{X}{\rightarrow} MeRe^{V}O(mtp)(OX) \xrightarrow{+L} MeRe^{V}O(mtp)L + XO \quad (2)$$

Step 2 of eq 1, elimination of Y, is rate-controlling. Here, we are focusing on the first step of eq 2, which remained

* To whom correspondence should be addressed. E-mail: espsenson@ameslab.gov.

(1) Zhang, C.; Guzei, I. A.; Espenson, J. H. *Inorg. Chem.* **2001**, *40*, 2437−2438.
(2) Arias, J.; Newlands, C. R.; Abu-Omar, M. M. *Inorg. Chem.* **2001**, *40*, 2185−2192.
(3) Wang, W.-D.; Espenson, J. H. *Inorg. Chem.* **2001**, *40*, 1323−1328.
(4) Huang, R.; Espenson, J. H. *J. Mol. Catal. A: Chem.* **2001**, *168*, 39−46.
(5) Huang, R.; Espenson, J. H. *Inorg. Chem.* **2001**, *40*, 994.
(6) Wang, W.-D.; Guzei, I. A.; Espenson, J. H. *Organometallics* **2001**, *20*, 148−156.
(7) Wang, Y.; Espenson, J. H. *Org. Lett.* **2000**, *2*, 3525−3526.
(8) Lente, G.; Espenson, J. H. *Inorg. Chem.* **2000**, *39*, 4809−4814.
(9) Lippard, S. J.; Berg, J. M. *Principles of Bioinorganic Chemistry*; University Science Books: Mill Valley, CA, 1994.
(10) Baird, D. M.; Aburri, C.; Barron, L. S.; Rodriguez, S. A. *Inorg. Chim. Acta* **1995**, *237*, 117−122.
(11) Caradonna, J. P.; Reddy, P. R.; Holm, R. H. *J. Am. Chem. Soc.* **1988**, *110*, 2139−2144.
(12) Holm, R. H.; Berg, J. M. *Acc. Chem. Res.* **1986**, *19*, 363−370.
(13) Holm, R. H. *Chem. Rev.* **1987**, *87*, 1401−1449.
(14) Li, H.; Palanca, P.; Sanz, V.; Lahoz, L. *Inorg. Chim. Acta* **1999**, *285*, 25−30.
(15) Laughlin, L. J.; Young, C. G. *Inorg. Chem.* **1996**, *35*, 1050−1058.
(16) Smith, P. D.; Millar, A. J.; Young, C. G.; Ghosh, A.; Basu, P. *J. Am. Chem. Soc.* **2000**, *122*, 9298−9299.
(17) Smith, P. D.; Slizys, D. A.; George, G. N.; Young, C. G. *J. Am. Chem. Soc.* **2000**, *122*, 2946−2947.
(18) Hille, R. *Chem. Rev.* **1996**, *96*, 2757−2816.
(19) Johnson, M. K.; Rees, D. C.; Adams, M. W. W. *Chem. Rev.* **1996**, *96*, 2817−2839.

10.1021/ic011166j CCC: $22.00
Published on Web 08/10/2002

Chart 1

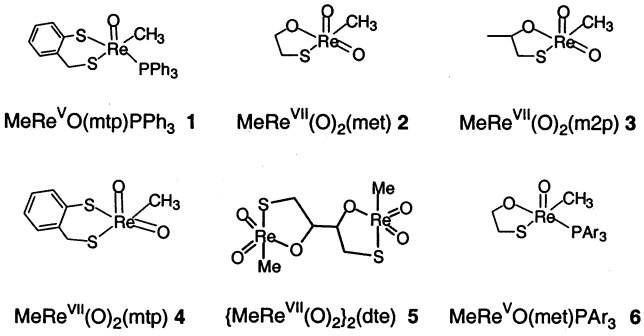

uncharacterized save for competition experiments, because **4** does not grow to a detectable concentration. For that reason, we synthesized compounds **2**, **3**, and **5** that were sufficiently stable for characterization and reactivity studies. As X in eq 2, this work has employed triphenylphosphane, methyl tolyl sulfide, and triphenylarsane.

Experimental Section

Preparation, Isolation, and Stability of 2, 3, and 5. These compounds were prepared from reactions between $MeReO_3$[23] and a 1,2-hydroxythiol in 1:1 proportions in methylene chloride under argon.

{MeReO$_2$}$_2$(dte), 5. Dithioerythritol (0.118 g, 0.77 mmol) was dissolved in 5 mL of methylene chloride and 10 mL of toluene which was heated and added all at once to the $MeReO_3$ solution. The mixture was stirred for 20 min in an ice bath and then stirred under ambient conditions for 5 h. The reaction mixture was transferred to a new flask, layered with hexane, and held at −22 °C for 5 days. Dark red crystals were collected by suction filtration, washed with 10 mL of hexanes, and dried. Compound **5** was isolated in pure form; it has been characterized crystallographically.[24] Elemental analysis: C, 11.88 found (11.69 calcd); H, 1.97 (1.96); S, 10.39 (10.40). ^{1}H NMR: δ 4.29 (m, 2H), 2.94 (m, 4H), 2.26 (s, 6H). ^{13}C NMR: δ 34.0, 33.1, 29.5, 19.6. UV−vis ($CHCl_3$), λ_{max}/nm, (log ϵ/L mol^{-1} cm^{-1}): 284 (2.10), 341(1.7), 425 (1.2, sh), and 350 (0.8, sh).

For the preparation of **2**, an oven-dried, three-necked flask equipped with a magnetic stirring bar was purged with a slow flow of argon, after which $MeReO_3$ (0.255 g, 1.00 mmol) was added and completely dissolved in 20−25 mL of methylene chloride; 1-mercaptoethanol (72 μL, 1.00 mmol) was then slowly added. The solution was stirred for 5 h under a slight flow of argon, as its color changed from colorless to a bright yellow and then to a deep red. The solvent was removed under vacuum, giving 0.312 g of **2** as a red oil. UV−vis ($CHCl_3$), λ_{max}/nm, (log ϵ/L mol^{-1} cm^{-1}): 334 (3.1), 410 (2.6, sh), and 500 (1.7, sh). ^{1}H NMR ($CDCl_3$): δ 5.04 (t, 2H, J = 6.3 Hz), 4.72 (t, 2H, J = 6.3 Hz), 2.52 (s, 3H), as displayed in Figure S-1. The NMR spectrum of the stock solution of **2** was the same before and after the kinetic studies. Efforts to obtain highly pure samples of **2** (and **3**) were thwarted by self-decomposition that intensified as solutions were concentrated, as put forth in Scheme 1.

Scheme 1. Concurrent Reactions of Dioxorhenium(VII) Complexes

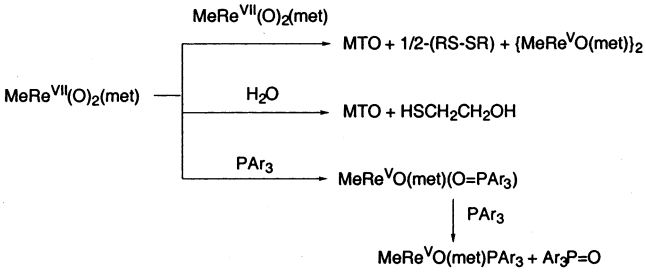

The method for **3** was essentially the same, using 1-mercapto-2-propanol (86 μL, 0.98 mmol); this reagent came in 95% purity, accompanied by 5% of 2-hydroxypropyl disulfide, yielding 0.31 g of **3** as a red oil, a 96% yield if **3** were pure. UV−vis ($CHCl_3$), λ_{max}/nm (log ϵ/L mol^{-1} cm^{-1}): 334 (3.0), 408 (2.6, sh), and 488 (2.5, sh). ^{1}H NMR ($CDCl_3$): δ 5.29 (m, 1H), 4.22 (dd, 1H, J 3.6 and 5.7 Hz), 3.82 (dd, 1H, J = 5.4 and 11.7 Hz), 2.48 (s, 3H, J = 2.4 Hz), as shown in Figure S-2.

By ^{1}H NMR, **2** was stable in $CDCl_3$ for several days when stored at −22 °C, or for >1 week when treated with at least an equimolar quantity of anhydrous magnesium sulfate. The NMR spectrum showed that **2** obtained by this procedure is 91% pure, the balance being 2-hydroxyethyl disulfide, $HO(CH_2)_2S-S(CH_2)_2OH$, and $MeReO_3$. In chloroform, **3** was rather more stable than **2**; also, **3** could be stored as an oil at 22 °C for >3 weeks without decomposition. Eventually, however, **3** decomposed to $MeReO_3$ and 2-hydroxypropyl disulfide. The product of the reaction between **2** and excess PPh_3, **6**, has the ^{1}H NMR spectrum presented in Figure S-3.

Dioxorhenium(VII) dithiolates decompose by an internal redox process; for example, for **4**

$$2MeRe(O)_2(mtp)\ (\mathbf{4}) + (L) \rightarrow MeReO_3 + MeReO(mtp)L\ [\text{or } {}^1/_2\{MeReO(mtp)\}_2] + RS{-}SR \quad (3)$$

where RS−SR is the five-membered ring disulfide resulting from the oxidation of the dithiolate and L is an incidental ligand (deliberately added Py or PZ_3, for example). This reaction is so rapid that no direct studies on **4** have been carried out. Indeed, the identity of **4** was inferred from the catalytic data and was confirmed independently by NMR experiments at −40 °C.[22] By means of kinetic competition, however, it could be shown that reaction 3 is *second-order* with respect to [**4**], whereas the desired reaction in catalysis between **4** and oxygen acceptor X is pseudo-first-order when a large excess of X was used. Irrespective of that, only kinetic competition data for **4** with PPh_3 were obtained because such reactions are quite rapid compared to other steps in the cycle that have a greater kinetic barrier.

Re(VII) compounds **2** and **3** are prone to similar second-order decomposition, so that the rate of decomposition increases as either compound is concentrated for purification. The reactions evidently involve water, in that the first two products in each equation have been explicitly identified:

$$2MeRe(O)_2(met)\ (\mathbf{2}) + H_2O \rightarrow MeReO_3 + \{HO(CH_2)_2S\}_2 + \{MeRe^V(met)\}_2 \quad (4)$$

$$2MeRe(O)_2(m2p)\ (\mathbf{3}) + H_2O \rightarrow MeReO_3 + \{HO(CHMeCH_2)S\}_2 + \{MeRe^V(m2p)\}_2 \quad (5)$$

Despite the lack of perfectly pure **2** and **3**, we elected to continue the studies, particularly with **2**, because such reactions are implicated

(20) Sung, K.-M.; Holm, R. H. *Inorg. Chem.* **2000**, *39*, 1275−1281.
(21) Sung, K.-M.; Holm, R. H. *J. Am. Chem. Soc.* **2001**, *123*, 1931−1943.
(22) Wang, Y.; Espenson, J. H. *Inorg. Chem.* **2002**, *41*, 2266−2274.
(23) Herrmann, W. A.; Kratzer, R. M.; Fischer, R. W. *Angew. Chem., Int. Ed. Engl.* **1997**, *36*, 2652−2654.
(24) Espenson, J. H.; Shan, X.; Wang, Y.; Huang, R.; Lahti, D. W.; Dixon, J.; Lente, G.; Ellern, A.; Guzei, I. A. *Inorg. Chem.* **2002**, *41*, 2583−2591.

Scheme 2. Reactions of $\{MeRe(O)_2\}_2(dte)$ (**5**) with PPh_3

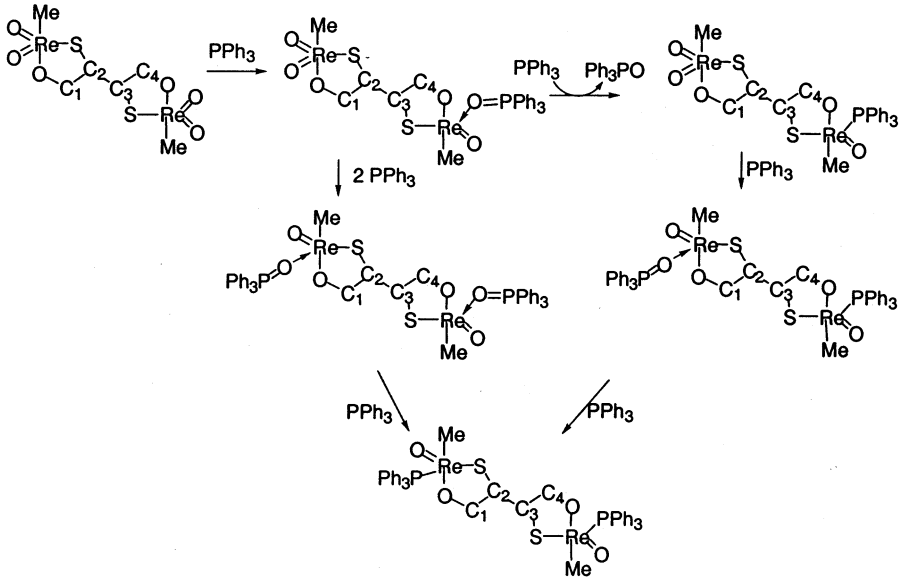

in catalysis. The byproducts $MeReO_3$ and the disulfides, coexisting with **2** and **3**, were shown to have no effect.

Data and Analysis. ^1H and ^{31}P NMR experiments were recorded with a Bruker DRX-400 MHz spectrometer**.** The kinetic data were obtained by a Shimadzu 3101 spectrophotometer, sometimes at ambient temperature (24 ± 1 °C), others with thermostatic control in the range 10−30 °C. Absorbance−time data were collected at 340 ± 1 nm for a series of experiments in which the phosphane concentrations were varied. The excess of phosphane was sufficient to allow data analysis by pseudo-first-order kinetics. Nonlinear analysis of the absorbance−time data, $Abs_t = Abs_\infty + (Abs_0 - Abs_\infty) \times \exp(-k_\psi t)$, was used to obtain values of k_ψ that varied linearly with the *first* power of $[PAr_3]$.

Results

Constitution of 2. The reactivity of **2** may be represented by the competing reactions presented in Scheme 1. The reactions between **2** and reagents X (= phosphanes, triphenylarsane, and methyl tolyl sulfide) are

$$MeRe^{VII}(O)_2(met)\ (\mathbf{2}) + X \rightarrow MeRe^{V}(O)(met)(OX) \quad (6)$$

$$MeRe^{V}(O)(met)(OX) + L\ (\text{or } X) \rightarrow MeRe^{V}(O)(met)L + XO$$

Reactions with Phosphanes. According to repetitive UV−vis scans, the reactions of PAr_3 with **2**, **3**, and **5** were complete in 30 min, most within 5 min. The 284 and 420 nm peaks of **5** (0.1 mM) decreased when PEt_3 (0.2−1.0 mM) was added, whereas the 345 nm peak increased as λ_{max} shifted to 350 nm. With PPh_3 or PEt_2OPh, the 284 nm peak of **5** decreased while that at 345 nm shifted slightly and intensified. After these initial changes, no changes in absorbance were detected with further PZ_3 beyond the 1:2 net stoichiometry of reaction 6.

For **2** and **3**, which themselves have strong absorptions in the 240−320 nm range, repetitive scans with PAr_3 reagents were performed in the range 330−370 nm. Single-wavelength kinetic data were then obtained by monitoring the absorbance increase at ca. 340 nm as the reaction progressed. All the reactions were complete in <5 min, except those with $P(C_6H_5CF_3)_3$, which required ∼25 min, and $P(C_6F_5)_3$, which failed to react.

In all cases, Ar_3PO was found by ^1H and ^{31}P NMR spectroscopy in an amount equal to the starting concentration of **2** or **3** within the precision of the measurement. New ^1H and ^{31}P signals were seen, consistent with the formation of **6** and MeReO(m2p)PAr_3, although neither compound was stable enough for isolation. Solutions for product detection were prepared in $CDCl_3$ with 112−129 mM PAr_3 and 46 mM **2**. The results established that the reaction between PAr_3 and **2** needs 2 phosphanes per rhenium to reach completion. Resonances at δ 2−6 ppm can be attributed to **6**. The phosphane ligand renders the protons of met diastereotopic, and they are seen separately, as listed in Table S-1.

NMR titrations of **5** with PPh_3 were carried out in benzene-d_6 at 3.5 mM **5** with P/Re ratios of 0.46−2.5. The solutions started as orange-red, turned deep red in the range 3.3−9.6 mM PPh_3, and became light blue at $[PPh_3] > 14.4$ mM (that is, at P/Re = 2). Numerous ^{31}P resonances were seen during the progression of this series of experiments. Scheme 2, which makes no effort to include detailed stereochemistry, shows some of the species involved, but likely not all of them. After 14.4 mM PPh_3, it and the Ph_3PO produced were the principal components.

Kinetic data obtained for reactions of **2** with triarylphosphanes are summarized in Table 1. Given the lower purity of **3**, it was examined only with PPh_3. The rate constants in Table 1 are defined according to the following rate law:

$$-\frac{d[Re(VII)]}{dt} = k_2[Re(VII)] \times [PAr_3] \quad (7)$$

Kinetic studies of $P(C_6H_4Cl)_3$ were carried out as a function of temperature. Analysis by the Eyring equation gave the following activation parameters: $\Delta S_{2Cl}^{\ddagger} = -214(21)$ J K^{-1} and $\Delta H_{2Cl}^{\ddagger} = 15.1(7)$ kJ (Figure S-4). The

Table 1. Summary of Reaction Conditions[a] and Rate Constants for Reactions between $MeRe(O)_2(met)$, **2**, and PAr_3

PAr_3	$[PAr_3]$ range (mmol/L)	k ($L\ mol^{-1}\ s^{-1}$)
$P(p\text{-}C_6H_4OMe)_3$	0.4−0.7	215(7)
$P(p\text{-}C_6H_4Me)_3$	0.4−0.7	180(2)
$P(p\text{-}C_6H_5)_3$	0.2−0.6	85.3(24)
$P(p\text{-}C_6H_4F)_3$	0.4−0.8	30.8(7)
$P(p\text{-}C_6H_4Cl)_3$	0.4−0.8	28.2(8)
$P(p\text{-}C_6H_4CF_3)_3$	0.4−0.8	4.79(15)
$P(C_6H_5)_3$	0.4−0.8	26.4(5)[b]

[a] At 24 ± 1 °C in chloroform, with 0.04 mM **2**, except 0.02 mM **2** for PPh_3; monitored at 348−350 nm. [b] The dioxorhenium(VII) compound is **3**.

relatively low value of $\Delta H_2^{\ddagger}$ (reflecting the mild dependence of k upon T) indicates that the main activation barrier is entropic.

Reactions with $AsPh_3$. No reaction was detected by ^1H NMR spectroscopy between **2** (40 mM) and triphenylarsane (100 mM) in $CDCl_3$ over 24 h. By that time, significant decomposition of **2** had begun, according to Scheme 1.

Reactions with *tert*-Butyl Hydroperoxide. Combination of **2** and TBHP directly gave no sign of a new intermediate but resulted in the conversion of TBHP to *tert*-butyl alcohol, TBA.[25]

$$MeRe(O)_2(met) + TBHP \rightarrow MeReO_3 + {}^1/_2\{HO(CH_2)_2S\}_2 + TBA \quad (8)$$

Reactions with Methyl Tolyl Sulfide. No reaction was found between the dioxorhenium(VII) complexes and MeSTol with these combinations: (a) **5** (13 mM) and MeSTol (27 mM) in benzene-d_6 for 20 h; (b) **2** (27 mM) and MeSTol (69 mM) in $CDCl_3$ for 20 h. The MeSTol remained completely unchanged, and in the second of these, **2** had begun its ordinary decomposition. When TBHP was also added, however, MeS(O)Tol and TBA were formed in a reaction that is stoichiometric and not catalytic under these conditions. Note that the reaction between TBHP and MeSTol under these conditions is nearly nonexistent in the absence of a catalyst. Taken together, these observations indicate that the reaction between **2** and MeSTol lies somewhat uphill and is drawn to completion as TBHP reacts with the oxorhenium(V) species so formed.

$$\mathbf{2} + 2MeSTol \leftrightharpoons MeReO(met)\{MeS(O)Tol)\} + MeS(O)Tol \quad (9)$$

Similarly, the combination of **5** (6.4 mM), MeSTol (27 mM), and TBHP (variable) leads to MeS(O)Tol, which it does not do without TBHP. The ^1H NMR spectra of MeS(O)Tol and unreacted MeSTol were evident until TBHP was added in excess, in which case only MeS(O)Tol could be detected. These are rapid transformations, complete within minutes.

(25) In this equation, RSSR represents the disulfide arising from the oxidation of $^-OCH_2CH_2S^-$ followed by reaction of $^-OCH_2CH_2S-SCH_2CH_2O^-$ with (presumably) water, giving $HOCH_2CH_2S-SCH_2CH_2OH$ and hydroxide/alkoxide ions. Details are not known.

Scheme 3. Catalytic Cycling for MTS Oxidation

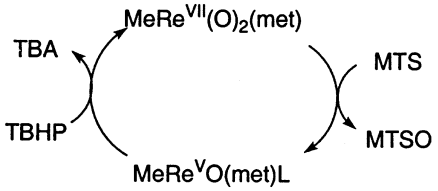

To test the premise that equilibrium in reaction 9 lies to the left (note the close balance in reactions of R_2S with $[Re(O)_2(hoz)_2]^+$, **7**, where hozH = 2-(2′-hydroxyphenyl)-2-oxazoline[2]), reactions were run with **2** (30 mM), $PTol_3$ (75 mM), and MeS(O)Tol (225 mM) in $CDCl_3$. In one case, **2** and $PTol_3$ were first mixed, and then, MeS(O)Tol was added. In the other, $PTol_3$ and MeS(O)Tol were added first, followed by **2**. Both reactions underwent similar color changes: red to blue-green (1−2 min) to green, and they arrived at the same final yellow color. The second reaction went more quickly, but both were complete within 30 min. The NMR spectra for the two were identical, with peaks corresponding to **2**, MeS(O)Tol, MeSTol, and Tol_3PO. The integrations of the methyl peaks of these compounds, given in Table S-2, are close to the values expected from this net equation, **2** being a catalyst, MeS(O)Tol + $PTol_3$ → MeSTol + Tol_3PO.

Oxygen atom transfer from TBHP to MeSTol is catalyzed by **2**. With MeSTol (14 mM), TBHP (14 mM), and **2** (0.14 mM) in $CDCl_3$, no change in the NMR spectrum could be detected after 10 min, but the reaction had gone to completion by 18 h. A slight amount of TBHP remained, no doubt a result of the initial concentrations not being precisely equal, but TBA was found at a concentration equivalent to that of the initial MeSTol. The concurrent use of TBHP and MeSTol sets up a catalytic cycle for MeSTol + TBHP → MeS(O)Tol + TBA, as in Scheme 3.

Discussion

Reactions with Phosphanes. The net reaction between **2** and phosphane is given by the directly determined stoichiometry, the sum of two steps in eq 6:

$$MeRe(O)_2(met) + 2PPh_3 = MeReO(met)(PPh_3) + PPh_3O \quad (10)$$

The kinetic data, including the first-order dependence on phosphane concentration, point to the first step in eq 6 as being rate-controlling. (An alternative, in which $MeRe^VO(OPPh_3)(met)$ rapidly builds up and then reacts completely with PPh_3, would also fit the kinetics, but it is not supported by the NMR spectroscopy because **2** remains at its full intensity.) Reaction 6 depicts phosphane attack at an oxo group; in effect, a phosphane oxide complex of rhenium(V) is formed. This proposal is consistent with the directly detected Mo←O═PPh_3 intermediate from which PPh_3 is later lost;[16] for another, it provides for displacement of phosphane oxide by phosphane. Such ligand displacement reactions have been extensively studied.[26] It appears quite unlikely that Ph_3PO is lost and PPh_3 then coordinated because that would be unprecedented: the Gibbs energy of a four-coordinate species

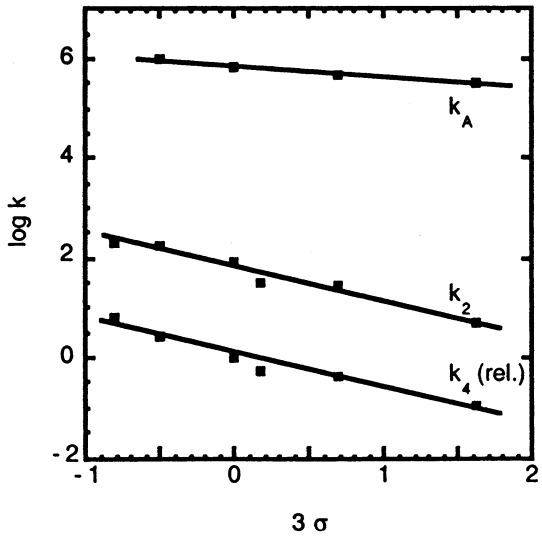

Figure 1. Analysis of kinetic data according to the method of Hammett, $\log(k) = \log(k_H) + \rho \times \sigma$, the latter being the Hammett substituent constant for group X. Data are shown for three reaction series in which P(*p*-$XC_6H_4)_3$ is converted to (*p*-$XC_6H_4)_3PO$. The *x*-axis shows 3σ because three equivalent aryl groups are present. The rate constants are k_2 (step 1, eq 6 with X = PAr_3 Table 1), k_4 (relative to $k_{4H} = 1.00$), and k_A, for $MeRe(O)_2(\kappa^2\text{-}O_2)\text{-}(H_2O)$.

such as MeReO(mtp), and now MeReO(met), makes them implausible intermediates. Indeed, when the system is in one way or another deprived of a ligand, or employs a ligand that is too weak a Lewis base, a dimer is formed (but not necessarily rapidly):[27]

$$2MeRe^{V}O(mtp)L \rightleftharpoons \{MeRe^{V}O(mtp)\}_2 + 2L \quad (11)$$

Competition experiments to characterize the reactivity of **4** gave rate constants designated in Table 1 as k_4(rel).[22] Figure 1 shows a plot of log *k* against 3σ, this being the Hammett substituent constant. Both k_2 and k_4(rel) show a good fit (correlation coefficients are $R = 0.980$ and 0.977, respectively). The reaction constants are $\rho = -0.69 \pm 0.07$ for each. Again, because of the normalization of k_4 to a relative value for PPh_3—by which is meant $k_{4H} = 1.000$ or $\log(k_{4H}) = 0$—this line appears on the graph below k_2; in actuality, the qualitative chemistry suggests that k_4 for a given PAr_3 is greater than k_2, perhaps much greater.

Figure 1 also presents the Hammett analysis of kinetic data for reactions between $MeRe(O)_2(\kappa^2\text{-}O_2)$, **A**,[28−30] and PAr_3. The reactions of **A** are much faster than those of **2** (note the absolute reactivity scale on the graph), but its substituent effect is milder, with $\rho_A = -0.21(2)$ against 3σ. Perhaps this is case of "more reactive−less selective", but more seems to come into play here. The reaction of **A** entails attack at the peroxo oxygen:[31]

$$PAr_3 + MeRe(O)_2(\kappa^2\text{-}O_2)\ (\mathbf{A}) \rightarrow Ar_3PO + MeReO_3 \quad (k_A) \quad (12)$$

We infer that the inherent weakness of the O—O bond as compared to Re═O accounts for the absolute reactivity difference, $k_A \gg k_2$. A Re═O bond has an oxygen atom that is positive relative to that of an oxygen atom in a peroxo-rhenium group. The inductive effect of the ring substituent on phosphane might therefore be less for the peroxo-rhenium case. Moreover, the reaction of **2** with PAr_3 does not proceed directly to free Ar_3PO, but to its rhenium(V) complex. A second point of comparison, suggested to us by a reviewer, is with the value $\rho = -4.5$ for the closely related **7**,[2] representing a greater difference that may arise from the positive charge on the latter species. As such, **7** can discriminate in reactivity among different phosphanes to a much greater extent.

Reaction with MeSTol. We have argued that eq 9 represents a reaction with a mildly positive value of $\Delta G°$; TBHP can evidently react with MeReO(met){MeS(O)Tol}, the species initially formed, drawing the reaction to the right. The steps that must ultimately balance are its components (both steps of eq 6, X = L = MeSTol) as well as the monomer−dimer equilibrium of eq 9, which is known to disfavor the monomer in the case of a poor Lewis base like a thioether.

Cationic complex **7** participates in an equilibrium analogous to reaction 9, except that it lies in favor of Re(V).[2] The reaction $[(hoz)_2Re(O)_2]^+ + H_2O = [(hoz)_2Re^{V}O(OH_2)]^+ + {}^1/_2O_2$ is characterized by $\Delta G° \leq 20$ kcal. The qualitative comparisons arrived at here, $\Delta G° \geq 20$ kcal, indicate that $[(hoz)_2Re(O)_2]^+$ is a better oxidizing agent than **2**.

Triphenylarsane. The failure of this reaction to proceed might arise from thermodynamics because $\Delta G°$ is ca. 30 kcal less favorable for E = P as compared to E = As. One must also consider the possibility of a substantially higher kinetic barrier for the arsane, considering its steric demand. We have been unable to resolve which factor is dominant.

Acknowledgment. This research was supported by the National Science Foundation under Grant 9982004. Some experiments were conducted with the use of the facilities of the Ames Laboratory.

Supporting Information Available: Figures and tables of NMR spectra and chemical shifts. This material is available free of charge via the Internet at http://pubs.acs.org.

IC011166J

(26) Lahti, D. W.; Espenson, J. H. *J. Am. Chem. Soc.* **2001**, *123*, 6014−6024.
(27) Lente, G.; Guzei, I. A.; Espenson, J. H. *Inorg. Chem.* **2000**, *39*, 1311−1319.
(28) Pestovsky, O.; van Eldik, R.; Huston, P.; Espenson, J. H. *J. Chem. Soc., Dalton Trans.* **1995**, 133.
(29) Espenson, J. H. *Chem. Commun.* **1999**, 479−488.
(30) Gable, K. P. *Adv. Organomet. Chem.* **1997**, *41*, 127−161.
(31) Abu-Omar, M. M.; Espenson, J. H. *J. Am. Chem. Soc.* **1995**, *117*, 272.